



Published in final edited form as:

J Immunol. 2015 February 15; 194(4): 1489–1502. doi:10.4049/jimmunol.1401880.

Natural IgM prevents autoimmunity by enforcing B cell central tolerance induction

Trang T. T. Nguyen^{*†}, Rebecca A. Elsner^{*‡}, and Nicole Baumgarth^{*†:‡:§:¶}

^{*}Center for Comparative Medicine, University of California, Davis, Davis, CA 95616

[†]Graduate Group in Immunology, University of California, Davis, Davis, CA 95616

[‡]Microbiology Graduate Group, University of California, Davis, Davis, CA 95616

[§]Dept. Pathology, Microbiology & Immunology, University of California, Davis, Davis, CA 95616

[¶]School of Veterinary Medicine, University of California, Davis, Davis, CA 95616

Abstract

It is unclear why selective deficiency in secreted (s)IgM causes antibody-mediated autoimmunity. We demonstrate that sIgM is required for normal B cell development and selection. The CD5⁺ B cells that were previously shown to accumulate in body cavities of sIgM^{-/-} mice are not B-1a cells, but CD19^{int}, CD43⁻, short-lived, BCR-signaling unresponsive anergic B-2 cells. Body cavity B-1 cells were more than 10-fold reduced, including VH11⁺ and phosphatidylcholine-specific B-1a cells, while splenic B-1 cells were unaffected and marginal zone B cells increased. Follicular B cells had higher turnover rates, survived poorly after adoptive transfer and were unresponsiveness to BCR stimulation in vitro. sIgM bound to B cell precursors and provided a positive signal to overcome a block at the pro/pre-B stage and during IGHV repertoire selection. Polyclonal IgM rescued B cell development and returned autoantibody levels to near normal. Thus, natural IgM-deficiency causes primary autoimmune disease by altering B cell development, selection and central tolerance induction.

Introduction

IgM is produced by all jawed vertebrates. It is the first isotype produced in ontogeny and the first immunoglobulin produced in response to an insult. Its pentameric structure is also unique among the other Ig isotypes, indicating its unique contributions to immunity and the host's interactions with its environment (1). Spontaneous "natural" IgM secretion occurs without external microbial stimulation (2, 3). Major sources of natural IgM in mice are B-1 cells situated in spleen and bone marrow, producing at least 80% of the circulating IgM (4, 5). Natural IgM-producing B-1 cells appear to be selected on self-antigens (6, 7) and exhibit dual reactivity to both self and common microbial antigens (1, 8, 9). This selection process might ensure the generation of evolutionary "useful" specificities (8). Indeed, natural antibodies appear to bind particularly to "altered" self-antigens, such as antigens expressed

on dead and dying cells, which is thought to allow the efficient removal of tissue debris, and thereby the removal of potential auto-antigens (1, 9–12).

Rapid T-independent IgM responses to systemic application of microbial components, such as lipopolysaccharide of gram negative bacteria, or polysaccharide antigens are induced by both B-1 (13, 14) and by marginal zone (MZ) B cells (15), which have a high propensity for rapid differentiation to IgM-secreting cells. Finally, most conventional B cell responses result in the initial production of IgM by early-activated B cells, prior to class-switch recombination to IgG, IgA or IgE (16). Early low-affinity IgM may facilitate antigen-deposition in the developing germinal centers (17).

Selective IgM deficiency is a little studied, relatively rare primary immunodeficiency of humans, reported to occur at a prevalence rate of 0.03% (18). Selective IgM-deficiency is often associated with recurrent infections (18), consistent with findings in sIgM-deficient mice ($\mu\text{s}^{-/-}$), which showed increased morbidity and mortality from various bacterial and viral infections (19–22). The data highlight the importance of both natural and antigen-induced IgM in immune protection from pathogen encounter.

Mechanistically less well understood is the observed development of autoantibodies against double-stranded DNA (12, 23) and the increased risk of autoimmune diseases such as arthritis and SLE in a subset of humans with selective IgM deficiency and in $\mu\text{s}^{-/-}$ mice (11, 12, 18). It has been argued that this is due to a break of peripheral B cell tolerance due to ineffective removal of cell debris in the absence of natural antibodies (1, 11, 12). This is consistent with the repertoire of self-specificities that preferentially bind to dead and dying self and other components of the altered self (24, 25). Yet, no studies to date have demonstrated such lack of self-antigen removal. Moreover, various BCR transgenic and knock-in mice have been generated over the last two decades, which express a highly restricted oligoclonal or even monoclonal B cells, and often lack B-1 cells and/or B-1 cell-derived IgM (26–29). These mice do not appear to suffer from autoimmune disease, indicating that autoantibody production in IgM-deficiency may have other underlying causes.

Positive and negative selection events during B cell development are critical for the elimination of self-reactive B cells. The fate of the developing B cells is strongly dependent on the strength of BCR interaction with self-antigens (30, 31). Autoreactive immature B cells may either i) undergo light-chain re-arrangement, i.e. change their antigen-specificity, ii) become anergic, i.e. unresponsive, and express the BCR-inhibitory surface molecule CD5, or iii) die via apoptosis (31, 32). Overall strengths of the selecting signals appear to determine also B cell subset selection. Relatively strong signals seem to favor development of B-1 and follicular (FO) B cells, weaker signals drive marginal zone (MZ) B cell development (33, 34).

Lack of sIgM may affect B cell development, possibly via expression of the recently identified Fc μ R (35–38). However, reported alterations appeared not only subtle but also difficult to reconcile: two independently-generated strains of $\mu\text{s}^{-/-}$ mice were reported to have increased numbers of MZ B and B-1 cells, but a normal FO B cell compartment (39,

40). The increased MZ B cell development in μ s^{-/-} mice may indicate that sIgM may affect B cell subset selection during development, and that in its absence overall strengths of the selecting signals is reduced, resulting in increases in the MZ B cell compartment. However, this is not consistent with the reported expansion of their B-1 cell compartment (40), which one would expect to be reduced and with a lack of effects on FO B cells.

In order to determine the causes of autoantibody production in selective IgM-deficiency we reexamined the previously generated μ s^{-/-} mice (40). Our findings demonstrate that the accumulation of autoantibodies is due to non-redundant effects of sIgM on B cell development and repertoire selection. Escape from central tolerance induction in the absence of sIgM explains the accumulation of anergic CD5⁺ CD43⁻ B-2 cells and the generation of autoantibodies and identifies sIgM as a non-redundant regulator of B cell selection.

Materials and Methods

Mice

Eight- to twelve-week-old female and male mice, C57BL/6J (wildtype WT; CD45.2, Igh-b), B6.SJL-Ptprc^a Pepc^b/BoyJ (CD45.1), B6.129S7-*Rag1*^{tm1Mom}/J, and B6.Cg-Igh^a Thy1^a Gpi1^a/J (Igh-a) mice were obtained from The Jackson Laboratory. Breeding pairs of B6.129S-sIgM^{-/-} (μ s^{-/-} CD45.2, Igh-a) mice were a kind gift from Dr. Frances Lund (University of Alabama, Birmingham). Heterozygous μ s^{+/-} mice were created by intercrossing μ s^{-/-} and C57BL/6J mice. Heterozygous CD45.1xCD45.2 F1 mice were created by intercrossing B6.SJL-Ptprc^a Pepc^b/BoyJ with C57BL/6J mice. Igh-a x Igh-b mice were created by intercrossing B6.Cg-Igh^a Thy1^a Gpi1^a/J (Igh-a) with C57BL/6J mice. All mice were kept in specific-pathogen free housing, in HVAC-filtered filter-top cages, screened for the absence of 17 common mouse pathogens (list available upon request). Mice were euthanized by overexposure to carbon dioxide.

To generate mixed bone marrow irradiation chimeras, single-cell suspensions of bone marrow from the femur and tibia of WT (wildtype, C57BL/6J) and μ s^{-/-} mice were injected i.v. at a 1:1 ratio into CD45.1xCD45.2 F1 mice lethally irradiated by exposure to a gamma-irradiation source (800rd). Similarly, WT and Fc μ R^{-/-} (CD45.2; kindly provided by Dr. Hiromi Kubagawa (University of Alabama at Birmingham).) mixed bone marrow chimeras were generated by injecting WT or Fc μ R^{-/-} bone marrow into lethal-irradiated CD45.1 mice. Chimeras were allowed to reconstitute for at least 7 weeks before used in experiments. All procedures and experiments involving animals were approved by the Animal Use and Care Committee of the University of California, Davis.

B cell reconstitution after sublethal irradiation

Groups of 4 WT and μ s^{-/-} mice were sublethally irradiated by whole body exposure to a gamma-irradiation source (350rd). The mice were allowed to reconstitute peripheral B cell compartments for 12 days. Frequencies of transitional B cells (CD93⁺) in bone marrow and spleen were determined by flow cytometry.

Transfer of sIgM

Groups of three or four μ s^{-/-} mice were injected i. p. with either 50 μ l WT serum, containing roughly 200 μ g IgM as assessed by ELISA, μ s^{-/-} serum, or 200 μ g monoclonal IgM (Sigma-Aldrich, clone MOPC-104E, specific for α -1,3-glucose) per mouse three times per week for 3 weeks to reconstitute sIgM. Control mice received PBS only.

Flow cytometry

Spleen and lymph node cells were obtained by grinding the organ between frosted ends of glass slides. Bone marrow was obtained by flushing fibula and tibia with medium using a 23 gauge needle. Single-cell suspensions were stained as previously described (41). Briefly, after Fc receptor blocking (anti-CD16/32 5 μ g/ml) for 20min on ice cells were stained with the following fluorochrome-conjugates: SA-Qdot 605, SA-APC, CD93-PE, CD80-PE, CD86-APC, CD45.1-PerCP Cy5.5PE, CD45R Cy7APC, CD3e-Cy55APC, BrdU-FITC (all BD Pharmingen), CD45.2-(Cy7APC, Cy7PE) (Biolegend), CD5-(biotin, Cy5PE), CD45R-(FITC, Cy7APC), FITC-labeled, phosphatidyl-choline-containing liposomes (PtC)-FITC, CD21-(FITC, biotin), CD23-(FITC, APC), CD43-(PE, Cy7APC), CD19-(Cy5PE, APC), CD21-Cy5.5PE, CD24-Cy5.5PE, BP-1-APC, IgD-Cy7PE, IgM-(Cy7APC, Cy55APC) (all in-house generated). Dead cells were excluded by live/dead-pacblue staining (Invitrogen). Staining for BrdU was done according to the manufacturer's protocols using a BD Pharmingen BrdU Flow Kit. To accurately set gates to identify CD5 and CD43 expressing cells, we used "fluorescence minus one" controls in which cells were stained with all reagents except anti-CD5 and anti-CD43, respectively. For *In vitro* sIgM binding, sIgM (SouthernBiotech, Clone 11E10, specific for Lipopolysaccharide) was conjugated to biotin and added to bone marrow and spleen cells for 1 hour at 4°C. Staining was revealed with SA-allophycocyanin. Dead cells were excluded by live/dead-PacBlue.

For cell cycle analysis, surface-stained splenocytes were fixed with 2.5% PFA, washed in PBS + 1% bovine serum albumin and stained with anti-Ki67-FITC and 7-AAD (BD Pharmingen) overnight at 4°C. FACS-analysis was done using a 15-parameter FACS-Aria (41), or a Fortessa (BD) equipped with 4 lasers and optics for 22-parameter analysis. Analysis was done using FlowJo (kind gift of Adam Treister).

FACS-sorting of live "non-dump", non-autofluorescent CD19⁺ B cell subsets was done using a FACS Aria (BD Biosciences). Sort gates were defined as follows: follicular B cells, CD21^{int} CD23⁺; marginal zone B cells, CD21^{hi} CD23⁻; anergic B cells, CD21^{int} CD23⁻. Sort gates for bone marrow CD45R⁺ CD43⁻ B cell precursors: Fraction D, IgD⁻ IgM⁻; Fraction E, IgD⁻ IgM⁺; Fraction F, IgD⁺ IgM⁺. Sorting purities were > 95%.

Magnetic B cell enrichment

Splenic B cells were enriched using a cocktail of depleting antibodies (CD90.2-biotin, Dx5-biotin, Gr-1-biotin) and anti-biotin Microbeads (Miltenyi Biotech) after Fc-blocking. CD23 negative (non-FO) B cells in the peritoneal cavity were enriched by adding anti-CD23-biotin to the above antibody cocktail. Nylon filtered splenocytes were separated using *auto*MACS (Miltenyi Biotech). Purities of enriched B cells were >90% as determined by subsequent FACS analysis.

In vitro B cell proliferation assay

FACS-purified MZ, FO and anergic, CD21^{int} CD23⁻ B cells from WT and μ s^{-/-} were labeled with 0.5 μ M CFSE in PBS at a concentration of 10^7 cells/ml for 20 minutes at 37°C, washed twice with PBS and cultured at 2.5×10^5 cells/well in the presence or absence of anti-IgM 20 μ g/ml medium (RPMI 1640, 292 μ g/ml L-glutamine, 100 μ g/ml penicillin/streptomycin, 10% heat-inactivated FCS, 0.03 M 2-ME) in 96-well round-bottom plates for 3 days at 37°C in 5% CO₂. FACS analysis was done to identify the number of dividing cells.

Testing for serum antinuclear Ab (ANA)

The method of ANA staining was adapted from previous publications (42). 3T3 cells (A31, generously provided by Dr. Peter Barry, UC Davis) were grown on glass slides overnight and fixed with acetone for 10 minutes. The slides were blocked with Fc block in 10% Fetal Calf serum/PBS buffer for 1h washed twice with PBS and once with washing buffers (PBS + 0.1% BSA + 1% NCS) then incubated with mouse serum in PBS for 2h (1:100 dilution for 2.5 months old mice and 1:1000 dilution for 8 months old mice). Staining was revealed using goat anti mouse IgG-biotin and SA-Alexa594, each incubated for 1h at room temperature. The 3T3 stained slides were washed with PBS for 5 min at least three times and mounted with Fluoromount-G (Southern Biotech). Images were collected with an Olympus BX61 microscope with an Olympus DP72 color camera and were processed by using MetaMorph (Molecular Devices) and ImageJ (NIH) software. Differential interference contrast (DIC) images were taken for outlining the cells. Compared images were collected at the same day and analyzed in the same way. The scale bars were from two images (20X and 40X) and applied to others.

ELISA

DNA-specific IgG was measured by ELISAs. 96-well plates (Maxisorb; Thermo Fisher Scientific) were coated with 10 μ g/ml dsDNA from calf thymus or 10 μ g/ml ssDNA (degraded dsDNA after heating at 94°C for 14 min in 1N NaOH) in PBS overnight. After blocking with PBS/1% heat inactivated calf serum/0.1% milk powder/0.05% Tween 20 for 1 h, 2-fold serially diluted serum in PBS was added for 2 h. Plates were washed, and Ab-binding was revealed using biotin-conjugated anti-IgG (Southern Biotech) followed by a streptavidin-HRP (Vector Laboratories, Burlingame CA) incubation for 1 h and then substrate (10 mg/ml 3,3',5,5'-tetramethylbenzidine in 0.05 mM citric acid, 3% hydrogen peroxide) for 20 min. Reactions were stopped with 1 N sulfuric acid, and absorbance was read at 450 nm and reference wavelength of 595 nm using a SpectraMax M5 (Molecular Devices). Relative units Ab levels were calculated by comparison to NZB mouse serum.

qPCR and qRT-PCR

DNA was isolated from sorted cells by DNeasy kit (Qiagen) and stored in the DNA storage buffer at -20°C until processed. IgHV regions were amplified by qPCR as described previously (43) in sybergreen buffer (Applied Biosystems). For qRT-PCR analysis of VH11 mRNA expression, total RNA from peritoneal cavity B cells was isolated with RNeasy (Qiagen) and stored in the RNA storage buffer (Ambion) at -80°C until processed. Complementary DNA was prepared by using random hexamers (Promega) with Super-

Script II Reverse Transcriptase (Invitrogen). Primer/Probe for IGVH11 were designed using the IDT software (IDT): forward primer GAAGTGCAGCTGTTGGAGA; reverse primer GTACAGGGTGCTCTTGTCATT. Relative expression was normalized to GAPDH (IDT).

Statistical Analysis

Statistical analysis was done using a two-tailed Student's t test. $P < 0.05$ was considered to show significant differences, * $p < 0.05$, ** $p < 0.005$, *** $p < 0.0005$.

Results

An unusual population of CD5^{+/-} CD21^{int} CD23⁻ B cells develops in μ s^{-/-} mice

Measurements of autoantibodies by ELISA in 10 week-old μ s^{-/-} and age-matched WT controls confirmed earlier reports on the generation of high-titers IgG autoantibodies against ds and ssDNA in μ s^{-/-} mice (Fig. 1 A, B) (12, 23). We also found increased anti-nuclear IgG antibodies (ANA), which further increased with age (Fig. 1C, D). Thus, selective IgM deficiency causes the development of autoantibodies against multiple self-antigens, which increase with age. Comparison of total serum IgG levels in WT and μ s^{-/-} mice as assessed by ELISA revealed no significant differences between the mouse strains at 3 months of age and only very modest increases at 8 months (Supplemental Fig. 1A). Similarly, the frequencies of IgG-secreting cells in the spleen as measured by ELISPOT and the frequencies of spleen CD19⁺ CD138⁺ plasma cells were not significantly different between these two mouse strains (Supplemental Fig. 1B/C) Thus, the difference in autoantibody production in μ s^{-/-} mice cannot be explained by differences in total IgG levels and instead suggest B cell repertoire differences.

Modest increases in MZ (39) and peritoneal cavity B-1 cells in μ s^{-/-} mice (40) were previously reported. We confirmed the increased frequencies of MZ B cells and a concomitant decrease in follicular (FO) B cells in μ s^{-/-} mice (Fig. 2A, B), but identified multiple additional defects. First, μ s^{-/-} mice had significantly reduced numbers of CD19⁺ B cells, especially in lymph nodes (Fig. 2A, B). Moreover, we noted an unusual population of CD21^{int} CD23⁻ CD19⁺ B cells in spleens and lymph nodes of μ s^{-/-} mice that was not present in WT mice and blurred the differentiation of MZ and FO B cells somewhat (Fig. 2A). Further analysis identified them as CD5^{+/-} CD21^{lo} CD23⁻ CD43⁻ CD45R^{hi} CD93⁻ (Fig. 2C). Despite expression of CD5 on some of these cells, they were not classical B-1a cells, as they were mostly CD43⁻ and CD5 expression levels of those expressing CD5 were lower and their expression of CD45R was higher compared to that of B-1a cells (Fig. 2C). They were not transitional B cells either, as they lacked expression of CD93. Based on their expression of CD80 and CD86 they appeared to be antigen-experienced. In WT mice, very few B cells fell into the CD21^{int} CD23^{neg} B cell gate. Those that did were either B-1: CD5⁺ CD21^{lo} CD23⁻ CD43⁺ CD45R^{lo} or transitional B cells: CD5⁻ CD21^{lo} CD23⁻ CD43⁻ CD45R^{hi} CD93⁺ (Fig. 2C, D). FO cells also showed phenotypic alterations in μ s^{-/-} mice. They expressed reduced levels of IgD and some seemed to express very low levels of CD5 based on comparison to control stains that did not include CD5 (Fig. 2D and data not shown). These dramatic changes of the peripheral B cell compartments suggested that sIgM is a non-redundant component required for normal B cell development and B cell subset

selection and/or maintenance. We therefore explored the relationship between the effects of IgM on the B cell compartment and the regulation of autoantibody production.

B cell development from μ s^{-/-} bone marrow precursors is rescued in the presence of sIgM

First we determined whether the B cell developmental changes in μ s^{-/-} mice could be normalized by the administration of sIgM. For that we injected polyclonal IgM purified from WT serum into μ s^{-/-} mice three times per week for three weeks. Transfer of sIgM resulted in significant increases in the frequencies of FO B cells and reduced frequencies of CD21^{int} CD23⁻ B cells in spleen and lymph nodes compared to mice receiving serum from μ s^{-/-} mice; a decrease that reached statistical significance in the lymph nodes (Fig. 3A). Due to the very short half-life of IgM (2 days) (44), the levels of circulating serum sIgM could not be normalized with this approach (Fig. 3B), which may explain why a more complete rescue of B cells was not achieved.

Therefore, to test for the development of B cells from precursors of μ s^{-/-} mice in the presence of normal levels serum IgM we generated mixed bone marrow chimeras, transferring WT (CD45.1) and μ s^{-/-} (CD45.2) bone marrow at a 1:1 ratio into lethally irradiated CD45.1 x CD45.2 (F1) recipients. The CD45.1/CD45.2 double-positive radio-resistant recipient cells were easily distinguished from the single-positive WT and μ s^{-/-} donor B cells in the host (Fig. 3C, second panel). Recipients of WT or mixed μ s^{-/-} WT bone marrow had similar serum IgM levels, while recipients of μ s^{-/-} bone marrow lacked sIgM (Fig. 3E). Precursors from μ s^{-/-} mice reconstituted roughly half of each B cell compartment in the mixed bone marrow chimeras (Fig. 3C, D). Frequencies and phenotypes of all major B cell subsets were normal (Fig. 3C, D and not shown). Furthermore, CD21^{int} CD23⁻ B cells did not develop in the mixed chimeras, but did develop in controls that received μ s^{-/-} bone marrow only and thus lacked IgM (Fig. 3C, E). Importantly, ANA antibody development was greatly reduced in mixed bone marrow chimeras, compared to mice receiving μ s^{-/-} bone marrow only. The latter generated measurable levels of ANA within 10 weeks after adoptive transfer (Fig. 3F). Thus, precursors of μ s^{-/-} mice have no inherent developmental defect in B cell development when raised in the presence of sIgM.

B-1 cell frequencies are strongly reduced in the peritoneal cavity of μ s^{-/-} mice but are maintained at normal numbers in the spleen

Increased in peritoneal cavity CD5⁺ CD45R⁺ B-1 cells had been reported for μ s^{-/-} mice (40). While our results confirmed increases in frequencies of CD5⁺ B cells (Fig. 4A), these cells were mostly CD43^{neg} CD45R^{hi} and CD19^{int}, i.e. did not represent classical CD43⁺ CD45R^{lo} CD19^{hi} B-1a cells of WT mice (Fig. 4A/B). The difference in CD43 staining shown (Fig. 4A/B) is highly significant (MFI 2,131 ± 556 on WT CD19⁺ IgM⁺ versus 195 ± 34 for μ s^{-/-} cells p<0.005). Also, the difference on CD45R expression was greatly significant (1758 ± 259 versus 3,727 ± 115, p <0.0001), as was the reduction in expression of CD19 (12,720 ± 1036 versus 8,920 ± 320, p <0.005). Therefore, CD19^{hi} CD45R^{lo} CD43⁺ i.e. classical B-1a (CD5⁺) and B-1b (CD5⁻) cells were greatly reduced in the peritoneal cavity of μ s^{-/-} mice (Fig. 4C). Further confirmation of a reduction in B-1 cells came from the analysis of phosphatidyl choline (PtC)-specific cells, a B-1a cell-restricted specificity (25, 45). PtC-binding CD5⁺ B cells made < 1.0% of CD19⁺ peritoneal cavity B

cells in μ s^{-/-} mice compared to nearly 10% in C57BL/6 and 15% in 129 WT controls (Fig. 4D and data not shown). Since PtC-binding B-1 cells in C57BL/6 and 129 mice preferentially use VH11 (46) we determined whether the lack of B-1 cells might be the outcome of altered B cell selection. Indeed, CD23⁻ peritoneal cavity B cells of μ s^{-/-} mice showed a near complete absence of VH11 mRNA compared to the high expression seen in WT mice (Fig. 4E). The strong reduction of B cells in the μ s^{-/-} peritoneal cavity was not due to increases in B-1 cell death (Supplemental Fig. 2). It did also not appear to be due to an increase in B-1 cell migration from the cavities to the spleen, and subsequent differentiation to antibody-secreting cells, as is often seen after activation of peritoneal cavity B-1 cells, as frequencies of ASC in the spleen were comparable between WT and μ s^{-/-} mice (Supplemental Fig. 1). Thus, lack of B-1 cells in the peritoneal cavity may suggest differences in B cell selection. In contrast, B-1 cell numbers in the spleen and lymph nodes were unaffected (Fig. 4F).

To determine whether peritoneal cavity B-1 cell development can be rescued by the presence of sIgM, we created heterozygous μ s^{-/-} (Igh-a) x C57BL/6 (Igh-b) mice. As B cells undergo allelic exclusion, each B cell expresses IgM either from the WT or μ s^{-/-} allele. Differences in IgM-allotype expression identified their origins. The sIgM levels in μ s^{+/-} sera were comparable to that of wildtype mice (data not shown) and heterozygous mice had normal frequencies of total and PtC-binding B-1 cells in peritoneal cavity (Fig. 4G). Furthermore, μ s^{-/-}-derived (Igh-a) and WT-derived (Igh-b) B cells were present at similar frequencies in bone marrow, spleen and peritoneal cavity (Fig. 4H). The CD5^{+/-} CD21^{int} CD23⁻ B cell population observed in μ s^{-/-} mice was absent from peritoneal cavity and spleen (data not shown) and IgG autoantibody levels against dsDNA (Fig. 4I), ssDNA (Fig. 4J) and ANA-specific autoantibodies (Fig. 4K) were strongly reduced in sera from 10 week-old μ s^{+/-} mice compared to age-matched μ s^{-/-} controls. The slight, but not statistically significant increases of autoantibodies in the heterozygous compared to the WT mice might be due to local concentrations of sIgM in the immediate vicinity of B cells in the bone marrow. In summary, sIgM is a non-redundant factor required for the normal development of B-2 cells and peritoneal cavity, but not splenic, B-1 cells.

μ s^{-/-} CD21^{int} CD23⁻ B cells are anergic

CD5 is a negative regulator of BCR signaling and its expression on conventional B cells has been previously linked to anergy (32). The expression of CD5 on some FO and CD21^{int} CD23⁻ B cells suggested the emergence of anergic B cells in μ s^{-/-} mice. Anergic B cells are relatively short-lived and are unresponsive to BCR-mediated stimulation (47). Indeed, B cell subsets in μ s^{-/-} mice, including MZ and FO B cells showed enhanced turnover compared to their WT counterparts as measured by enhanced BrdU incorporation (Fig. 5A), as noted by others (48). The turnover-rate of CD21^{int} CD23⁻ B cells was similar to that of FO B cells in μ s^{-/-} mice, but enhanced compared to those in WT mice (Fig. 5A) and their rate of cell death, as measured by 7-AAD-incorporation, was highest among all B cell populations (Fig. 5B).

To determine whether the higher rate of BrdU incorporation was due to reduced B cell survival in μ s^{-/-} mice, we transferred equal numbers of CFSE-labeled splenic B cells from

WT (CD45.1) and μ s^{-/-} (CD45.2) into WT mice. All B cell subsets from μ s^{-/-} mice, including the CD5^{+/-} CD21^{int} CD23⁻ cells survived poorly compared to WT B cells at both two and 25 days after transfer (Fig. 5C, D). In addition, μ s^{-/-} mice had increased frequencies of B cells expressing the proliferation marker Ki67, as well as increased frequencies of CD19⁺ cells in the G1 phase of the cell cycle, compared to WT cells (Fig. 5E). Transfer of either sIgM containing WT serum or polyclonal IgM could reverse these increases, while monoclonal IgM could not (Fig. 5E, F).

We tested whether the reduced ability of μ s^{-/-} B cells to survive in vivo could be due to a lack of BCR-mediated signaling, as unresponsiveness to BCR signaling is a hallmark of anergic B cells and continuous “tonic” signaling through the BCR is required for B cell survival. Indeed, all B cell subsets from μ s^{-/-} mice showed greatly reduced proliferation in response to anti-IgM stimulation compared to their WT counterparts. The CD21^{int}CD23⁻CD5^{+/-} B cells appeared least responsive (Fig. 5G). Thus, B cells from μ s^{-/-} mice have a shortened lifespan and are hypo-responsive to BCR stimulation suggesting that a lack of sIgM leads to the development of anergic B cells.

Lack of sIgM causes alterations in B cell development

Given that the transfer of mature μ s^{-/-} B cells into a sIgM-complete environment could not rescue μ s^{-/-} B cell survival (Fig. 5D), sIgM might affect very early stages of B cell development. Analysis of bone marrow precursors showed that early pro B cells (Hardy scheme, Fraction (Fr.) A) and pro B cells (Fr. B) were increased in μ s^{-/-} compared to WT mice, but reduced after the pre-B cell stage (Supplemental Fig. 3A and Fig. 6A). Staining for CD93 expression on Hardy Fr. E further demonstrated a strong reduction of immature B cells in the bone marrow (Fig. 6A). Because reduced BCR-expression might affect identification of immature B cells (usually done via IgM/IgD staining) we added staining for CD93 to the analysis, which confirmed the decrease of immature B cells in μ s^{-/-} mice (Fig. 6A).

The rate of proliferation among pre-pro and late pre-B cells was similar between μ s^{-/-} and WT mice (Fig. 6B). Thus, the increases of Fr. A and B were not due to their increased expansion, but likely due to increased accumulation due to reduced progression through the pre-B cell stage. Consistent with the presence of reduced B cell precursors in the bone marrow, frequencies of splenic transitional B cells were reduced at transitional stage T1, but not at T2 in μ s^{-/-} compared to WT mice (Fig. 6C, Supplemental Fig. 3B). Finally, to directly compare bone marrow output, we assessed peripheral B cell reconstitution on day 12 after sublethal irradiation of μ s^{-/-} and WT mice. The results showed significant reductions in the frequencies (Fig. 6D) and total numbers (not shown) of immature/transitional CD19⁺ CD93⁺ B cells in the bone marrow and spleen of μ s^{-/-} mice compared to their wildtype controls. We conclude that the presence of secreted IgM, is required for normal bone marrow B cell development.

sIgM binds to bone marrow B cells

The data thus suggest that bone marrow B cell development is dependent on the presence of sIgM. To determine whether sIgM can bind to bone marrow B cells, and thus to assess

whether sIgM-B cell precursor-direct interaction may be responsible for the effect of sIgM on B cell development, we measured the binding of sIgM to B cells in bone marrow and periphery. Staining for total surface IgM, thus bound sIgM as well as membrane-bound BCR, showed that immature B cells from μ s $^{-/-}$ showed reduced IgM staining compared to WT controls (Fig. 6E). To distinguish surface IgM-expression from binding of sIgM to B cells via Fc or other receptors, which would not occur in μ s $^{-/-}$ mice, we created heterozygous Igh-a x Igh-b mice, in which the expressed IgM-allele and surface-bound IgM from the non-expressed allele were differentiated by surface staining with allotype-specific anti-IgM^a and anti-IgM^b. All B cells stained significantly for the non-expressed Igh-allotype, with stronger surface binding on peripheral B cells compared to bone marrow precursors (Fig. 6F), which explained the reduced staining for total surface IgM in μ s $^{-/-}$ compared to WT mice (Fig. 6E). Also, *in vitro* exposure of spleen and bone marrow cells to sIgM showed strong sIgM binding to B cells, particularly B cells from μ s $^{-/-}$ mice (Fig. 6G), including immature and mature B cells, but little to other cell types (Fig. 6G and Supplemental Fig. 4). We conclude that sIgM binds to B cells and their precursors *in vivo*.

Fc μ R $^{-/-}$ B cells show no defect in B cell development

Of the known surface IgM receptors, only the Fc μ R is expressed by early B cell precursors (35, 37) and we aimed to assess its effects on B cell development. First we tested for its contribution to sIgM binding to B cells and non-B cells. For that we exposed *in vitro* IgM labeled with biotin to bone marrow and spleen cells from bone-marrow irradiation chimeras generated by reconstituting wildtype C57BL/6 (CD45.1) mice with bone marrow from either wildtype C57BL/6 mice, or from Fc μ R $^{-/-}$ mice. Wildtype and Fc μ R $^{-/-}$ B cells were able to bind sIgM on their cell surface. The lack of the Fc μ R led to a measurable but only very modest reduction in sIgM-binding to B cells of bone marrow and spleen, while non-B cells showed no discernable IgM binding (Fig. 7A/B).

To determine whether direct binding of IgM via the Fc μ R might regulate B cell development, we studied the effects B cell development in these bone-marrow irradiation chimeras. Bone marrow B cell development appeared normal (Fig. 7C) and peripheral B cell subset composition in the spleen was similar to that of wildtype but not μ s $^{-/-}$ mice. An exception was the significant reduction in MZ B cells (Fig 7D/E), while total serum IgM levels were increased in chimeras reconstituted with Fc μ R $^{-/-}$ bone marrow compared to that of wildtype-reconstituted mice (Fig. 7F). These findings were similar to the original reports with this strain of Fc μ R $^{-/-}$ mice (53).

In vitro responses to anti-IgM stimulation were comparable between Fc μ R $^{-/-}$ B cells and wildtype B cells, while the μ s $^{-/-}$ B cells showed significant reduced B cell proliferation (Fig. 7G/H). Thus, sIgM direct-binding to B cells via the Fc μ R cannot explain the significant effects of sIgM on bone marrow B cell development. Since the lack of Fc μ R-expression reduced, but did not abrogate sIgM binding to B cells (Fig. 7A), the presence of other IgM-binding proteins on the surface of the developing B cells may regulate B cell development.

sIgM affects B cell repertoire and selection

The observed binding of sIgM onto B cell precursors may alter B cell selection at the immature B cell stage and with it the B cell repertoire. Comparison of the BCR repertoire of μ s^{-/-} and WT mice using qPCR on FACS-purified B cell fractions taken at different checkpoints during bone marrow B cell development showed significant differences in VH usage among bone marrow fractions D and E from μ s^{-/-} and WT mice (Fig. 8A, B). Mature B cells in the bone marrow and follicular B cells in periphery showed similar repertoire differences (Fig. 8C). Comparison of IGHV usage among FO B cells between WT and μ s^{-/-} mice and the CD21^{int} CD23⁻ B cells in μ s^{-/-} mice also revealed repertoire differences demonstrating the strong effects of sIgM on development of all B cell compartments (Fig. 8D). Combined with the findings of increased autoantibody generation in μ s^{-/-} mice, and reduced VH11 gene usage among B-1 cells, the data demonstrate that the lack of sIgM causes repertoire changes in both the B-1 and the B-2 cell compartments.

Discussion

The study revealed profound effects of sIgM on the development of most B cells and B cell subsets, thereby providing a mechanism through which sIgM prevents autoantibody formation, namely by facilitating normal B cell development and enforcing negative selection of autoreactive B cells. While the lack of auto-antigen clearance may contribute to autoantibody development in μ s^{-/-} (1, 9–12), the observed effects of sIgM on B cell development in bone marrow and periphery, and the reversal of autoantibody production following the reestablishment of normal B cell development suggests that these effects are the major underlying cause for the development of autoreactive B cells in IgM-deficiency.

The direct binding of sIgM to B cells, which we observed at all stages of B cell development from the pre-B cell stage onwards (Fig. 6E, F and data not shown), may provide the non-redundant signal for B cell development and selection. Among the three known B cell sIgM receptors, neither the Fc α / μ R nor the complement receptors CR1/2 are expressed on pro-, pre-B cells, and immature B cells (49–51), thus cannot be responsible for the observed effects of IgM deficiency. Fc μ R is expressed early in B cell development and was a potential candidate receptor for IgM (37, 52). In support, mice lacking the Fc μ R^{-/-} develop autoantibodies despite harboring normal levels serum sIgM (37, 52), further suggesting a central role for sIgM in regulation of B cell development rather than removal of auto-antigens for the enforcement of central tolerance induction. However, studies with bone marrow Fc μ R^{-/-} chimeras (Fig. 7), failed to reveal B cell developmental defects similar to those observed in the μ s^{-/-} mice. The phenotype of the bone marrow irradiation chimera is consistent with the original description of the Fc μ R^{-/-} mice from which we obtained the bone marrow (37). In those mice, overall B cell development was found to be unaffected, except for the reduction in MZ B cells and an increase in splenic B-1 cells as well as increases in serum IgM. A second report with independently generated Fc μ R^{-/-} mice reported no B cell abnormalities (49). However, a third group who generated Fc μ R^{-/-} mice reported reduction in all B cell precursors in the bone marrow, except mature Fraction F B cells. In contrast to our findings with the sIgM^{-/-} mice, they found increased numbers of peritoneal cavity B-1 cells in the Fc μ R^{-/-} mice (38). Thus, based on published work with

three different $Fc\mu R^{-/-}$ mice, the lack of this receptor appears to have some effects on B cell development. Those reported changes are more subtle and/or different from those shown here with the $sIgM^{-/-}$ mice. Most prominently, the accumulation of $CD5^{+/-}$ $CD43^{-}$ $CD23^{-}$ $CD21^{int}$ anergic B cell population in the $\mu s^{-/-}$ mice is not noted in any reports of the $Fc\mu R^{-/-}$ mice, nor was it found in the $Fc\mu R^{-/-}$ bone-marrow chimeras we created (Fig. 7). Given the somewhat contradictory reports on the phenotype of the three independently generated $Fc\mu R^{-/-}$ mice, compensatory mechanisms may make any differences on B cell development less obvious than a complete lack of $sIgM$. Alternatively, the various approaches that were taken in targeting the $Fc\mu R$, might have led to the differences in the effects. A direct comparison between the different gene-targeted mice could help to resolve some of these issues.

Since natural, polyclonal, but not monoclonal IgM rescued B cell development (Fig. 5F), our data indicate that natural IgM either directly or indirectly enhances BCR signaling strengths and thereby alters B cell central tolerance induction at the pre-B and immature B cell stage, possibly by facilitating auto-antigen presentation, as natural IgM -secreting cells appear selected on and directed against self-antigens (6). Yet, BCR-ligand-requirement for pre-B cell selection has not been documented (54). Alternatively, $sIgM$ may provide a co-stimulatory signal more akin to that provided by PRR, increasing responsiveness of the developing B cell to self-antigens. In support of a model in which $sIgM$ affects BCR signaling strengths, the lack of $sIgM$ altered the peripheral B cell VH -repertoire (Fig. 8), thus B cell selection, and led to the accumulation of autoantibody-secreting cells as well as to the presence of $CD5^{+/-}$ anergic and auto-reactive B cells in the periphery, possibly in an attempt to silence these auto-reactive cells. Together the data provide evidence that B cell-signaling and negative B cell selection at the immature B cell stage are defective in the absence of $sIgM$. The increases in MZ, decreases in FO and body cavity B-1 cells are also all consistent with reduced BCR-mediated signaling in $\mu s^{-/-}$ mice (33, 34).

Our findings of reduced peritoneal cavity B-1 cell frequencies in the $\mu s^{-/-}$ mice are opposite to conclusions drawn previously by others (40) but explained by the presence of $CD5^{+}$ $B220^{+}$ anergic B cells in the peritoneal cavity and spleen, which were likely misidentified as B-1a cells. Their lack of $CD43$ -expression, high expression of $B220$, intermediate expression of $CD19$, lack of $VH11$ -expression, and of PtC-binding are not consistent with emergence from the B-1 cell lineage. Furthermore, their turnover was amongst the highest of any B cells studied (Fig. 5), while B-1 cell turnover in the peritoneal cavity is very low (55, 56). Multiple mouse models have demonstrated that reduction in BCR-signaling strength reduces peritoneal cavity B-1 cell development (7). Thus, the demonstration of curtailed B-1 cell development in the $\mu s^{-/-}$ mice further supports a model in which $sIgM$ acts as a positive co-stimulatory signal during B cell development.

A “chicken and egg” problem emerges from the fact that $sIgM$ is required for normal B cell development but that it is not usually transmitted from the maternal circulation to the fetus. Thus, the development of fetal IgM secreting cells must not require IgM . Since B-1 cell numbers in the spleen were largely unaffected in $\mu s^{-/-}$ mice (Fig. 4), they might be the earliest source of natural IgM supporting further $sIgM$ -dependent B-1 and B-2 cell development. This is consistent with studies showing profound reductions in peritoneal

cavity B-1 cells after splenectomy (57) and with studies indicating that B-1 cell development arises in waves (58). Splenic B-1 cells may arise as a first wave of “IgM-independent” B-1 cells during fetal development, whereas body cavity B-1 cells emerge later and develop in a sIgM-dependent manner. The data indicate a new, non-redundant role for splenic B-1 cells in the regulation of B-2 cell development.

In summary, the study demonstrates that B-1 cells produce natural IgM to regulate B cell development and selection, thereby suppressing the development of autoreactive B cells. Identification of natural IgM as critical enforcer of central selection indicates these proteins as potential therapeutics against antibody-mediated autoimmune diseases.

Supplementary Material

Refer to Web version on PubMed Central for supplementary material.

Acknowledgments

This work was supported by NIH AI51354 and NIH AI85568, the Graduate Group in Immunology, UC Davis, and a Vietnamese Education Fellowship to T.T.T.N.

We thank Abigail Spinner and Frank Ventimiglia (California National Primate Research Center, UC Davis) for help with flow cytometry and assistance with cell imaging, respectively, and Adam Treister for FlowJo software. Special thanks to Dr. Frances Lund and Hiromi Kubagawa (University of Alabama at Birmingham) for generously sharing the sIgM^{-/-} mice and FcμR^{-/-} bone marrow, respectively, for these studies.

References

1. Ehrenstein MR, Notley CA. The importance of natural IgM: scavenger, protector and regulator. *Nature reviews Immunology*. 2010; 10:778–786.
2. Hooijkaas H, van der Linde-Preesman AA, Benne S, Benner R. Frequency analysis of the antibody specificity repertoire of mitogen-reactive B cells and “spontaneously” occurring “background” plaque-forming cells in nude mice. *Cellular immunology*. 1985; 92:154–162. [PubMed: 2416479]
3. Van Oudenaren A, Haaijman JJ, Benner R. Frequencies of background cytoplasmic Ig-containing cells in various lymphoid organs of athymic and euthymic mice as a function of age and immune status. *Immunology*. 1984; 51:735–742. [PubMed: 6231241]
4. Choi YS, Dieter JA, Rothausler K, Luo Z, Baumgarth N. B-1 cells in the bone marrow are a significant source of natural IgM. *European journal of immunology*. 2012; 42:120–129. [PubMed: 22009734]
5. Benner R, Hijmans W, Haaijman JJ. The bone marrow: the major source of serum immunoglobulins, but still a neglected site of antibody formation. *Clinical and experimental immunology*. 1981; 46:1–8. [PubMed: 7039877]
6. Hayakawa K, Asano M, Shinton SA, Gui M, Allman D, Stewart CL, Silver J, Hardy RR. Positive selection of natural autoreactive B cells. *Science*. 1999; 285:113–116. [PubMed: 10390361]
7. Berland R, Wortis HH. Origins and functions of B-1 cells with notes on the role of CD5. *Annual review of immunology*. 2002; 20:253–300.
8. Baumgarth N, Tung JW, Herzenberg LA. Inherent specificities in natural antibodies: a key to immune defense against pathogen invasion. *Springer seminars in immunopathology*. 2005; 26:347–362. [PubMed: 15633017]
9. Vas J, Gronwall C, Marshak-Rothstein A, Silverman GJ. Natural antibody to apoptotic cell membranes inhibits the proinflammatory properties of lupus autoantibody immune complexes. *Arthritis and rheumatism*. 2012; 64:3388–3398. [PubMed: 22577035]

10. Ogden CA, Kowalewski R, Peng Y, Montenegro V, Elkon KB. IGM is required for efficient complement mediated phagocytosis of apoptotic cells in vivo. *Autoimmunity*. 2005; 38:259–264. [PubMed: 16206508]
11. Notley CA, Brown MA, Wright GP, Ehrenstein MR. Natural IgM is required for suppression of inflammatory arthritis by apoptotic cells. *Journal of immunology*. 2011; 186:4967–4972.
12. Boes M, Schmidt T, Linkemann K, Beaudette BC, Marshak-Rothstein A, Chen J. Accelerated development of IgG autoantibodies and autoimmune disease in the absence of secreted IgM. *Proceedings of the National Academy of Sciences of the United States of America*. 2000; 97:1184–1189. [PubMed: 10655505]
13. Alugupalli KR, Gerstein RM, Chen J, Szomolanyi-Tsuda E, Woodland RT, Leong JM. The resolution of relapsing fever borreliosis requires IgM and is concurrent with expansion of B1b lymphocytes. *Journal of immunology*. 2003; 170:3819–3827.
14. Haas KM, Poe JC, Steeber DA, Tedder TF. B-1a and B-1b cells exhibit distinct developmental requirements and have unique functional roles in innate and adaptive immunity to *S. pneumoniae*. *Immunity*. 2005; 23:7–18. [PubMed: 16039575]
15. Martin F, Kearney JF. B-cell subsets and the mature preimmune repertoire. Marginal zone and B1 B cells as part of a “natural immune memory”. *Immunological reviews*. 2000; 175:70–79. [PubMed: 10933592]
16. Cebra JJ, Komisar JL, Schweitzer PA. CH isotype ‘switching’ during normal B-lymphocyte development. *Annual review of immunology*. 1984; 2:493–548.
17. Victora GD, Nussenzweig MC. Germinal centers. *Annual review of immunology*. 2012; 30:429–457.
18. Louis AG, Gupta S. Primary selective IgM deficiency: an ignored immunodeficiency. *Clinical reviews in allergy & immunology*. 2014; 46:104–111. [PubMed: 23760686]
19. Baumgarth N, Herman OC, Jager GC, Brown LE, Herzenberg LA, Chen J. B-1 and B-2 cell-derived immunoglobulin M antibodies are nonredundant components of the protective response to influenza virus infection. *The Journal of experimental medicine*. 2000; 192:271–280. [PubMed: 10899913]
20. Boes M, Prodeus AP, Schmidt T, Carroll MC, Chen J. A critical role of natural immunoglobulin M in immediate defense against systemic bacterial infection. *The Journal of experimental medicine*. 1998; 188:2381–2386. [PubMed: 9858525]
21. Choi YS, Baumgarth N. Dual role for B-1a cells in immunity to influenza virus infection. *The Journal of experimental medicine*. 2008; 205:3053–3064. [PubMed: 19075288]
22. Ochsenbein AF, Fehr T, Lutz C, Suter M, Brombacher F, Hengartner H, Zinkernagel RM. Control of early viral and bacterial distribution and disease by natural antibodies. *Science*. 1999; 286:2156–2159. [PubMed: 10591647]
23. Ehrenstein MR, Cook HT, Neuberger MS. Deficiency in serum immunoglobulin (Ig)M predisposes to development of IgG autoantibodies. *The Journal of experimental medicine*. 2000; 191:1253–1258. [PubMed: 10748243]
24. Rowley B, Tang L, Shinton S, Hayakawa K, Hardy RR. Autoreactive B-1 B cells: constraints on natural autoantibody B cell antigen receptors. *Journal of autoimmunity*. 2007; 29:236–245. [PubMed: 17889506]
25. Mercolino TJ, Arnold LW, Hawkins LA, Haughton G. Normal mouse peritoneum contains a large population of Ly-1+ (CD5) B cells that recognize phosphatidyl choline. Relationship to cells that secrete hemolytic antibody specific for autologous erythrocytes. *The Journal of experimental medicine*. 1988; 168:687–698. [PubMed: 3045250]
26. Erikson J, Radic MZ, Camper SA, Hardy RR, Carmack C, Weigert M. Expression of anti-DNA immunoglobulin transgenes in non-autoimmune mice. *Nature*. 1991; 349:331–334. [PubMed: 1898987]
27. Goodnow CC, Crosbie J, Adelstein S, Lavoie TB, Smith-Gill SJ, Brink RA, Pritchard-Briscoe H, Wotherspoon JS, Loblay RH, Raphael K, et al. Altered immunoglobulin expression and functional silencing of self-reactive B lymphocytes in transgenic mice. *Nature*. 1988; 334:676–682. [PubMed: 3261841]

28. Ota T, Doyle-Cooper C, Cooper AB, Doores KJ, Aoki-Ota M, Le K, Schief WR, Wyatt RT, Burton DR, Nemazee D. B cells from knock-in mice expressing broadly neutralizing HIV antibody b12 carry an innocuous B cell receptor responsive to HIV vaccine candidates. *Journal of immunology*. 2013; 191:3179–3185.
29. Nemazee DA, Burki K. Clonal deletion of B lymphocytes in a transgenic mouse bearing anti-MHC class I antibody genes. *Nature*. 1989; 337:562–566. [PubMed: 2783762]
30. Hardy RR, Hayakawa K. B cell development pathways. *Annual review of immunology*. 2001; 19:595–621.
31. von Boehmer H, Melchers F. Checkpoints in lymphocyte development and autoimmune disease. *Nature immunology*. 2010; 11:14–20. [PubMed: 20016505]
32. Hippen KL, Tze LE, Behrens TW. CD5 maintains tolerance in anergic B cells. *The Journal of experimental medicine*. 2000; 191:883–890. [PubMed: 10704468]
33. Pillai S, Cariappa A. The follicular versus marginal zone B lymphocyte cell fate decision. *Nature reviews. Immunology*. 2009; 9:767–777.
34. Casola S, Otipoby KL, Alimzhanov M, Humme S, Uyttersprot N, Kutok JL, Carroll MC, Rajewsky K. B cell receptor signal strength determines B cell fate. *Nature immunology*. 2004; 5:317–327. [PubMed: 14758357]
35. Kubagawa H, Oka S, Kubagawa Y, Torii I, Takayama E, Kang DW, Gartland GL, Bertoli LF, Mori H, Takatsu H, Kitamura T, Ohno H, Wang JY. Identity of the elusive IgM Fc receptor (FcmuR) in humans. *The Journal of experimental medicine*. 2009; 206:2779–2793. [PubMed: 19858324]
36. Shima H, Takatsu H, Fukuda S, Ohmae M, Hase K, Kubagawa H, Wang JY, Ohno H. Identification of TOSO/FAIM3 as an Fc receptor for IgM. *International immunology*. 2010; 22:149–156. [PubMed: 20042454]
37. Choi SC, Wang H, Tian L, Murakami Y, Shin DM, Borrego F, Morse HC 3rd, Coligan JE. Mouse IgM Fc receptor, FCMR, promotes B cell development and modulates antigen-driven immune responses. *Journal of immunology*. 2013; 190:987–996.
38. Ouchida R, Mori H, Hase K, Takatsu H, Kurosaki T, Tokuhisa T, Ohno H, Wang JY. Critical role of the IgM Fc receptor in IgM homeostasis, B-cell survival, and humoral immune responses. *Proceedings of the National Academy of Sciences of the United States of America*. 2012; 109:E2699–2706. [PubMed: 22988094]
39. Baker N, Ehrenstein MR. Cutting edge: selection of B lymphocyte subsets is regulated by natural IgM. *Journal of immunology*. 2002; 169:6686–6690.
40. Boes M, Esau C, Fischer MB, Schmidt T, Carroll M, Chen J. Enhanced B-1 cell development, but impaired IgG antibody responses in mice deficient in secreted IgM. *Journal of immunology*. 1998; 160:4776–4787.
41. Rothausler K, Baumgarth N. Evaluation of intranuclear BrdU detection procedures for use in multicolor flow cytometry. *Cytometry A*. 2006; 69:249–259. [PubMed: 16538653]
42. Yamamoto T, Takagawa S, Katayama I, Yamazaki K, Hamazaki Y, Shinkai H, Nishioka K. Animal model of sclerotic skin. I: Local injections of bleomycin induce sclerotic skin mimicking scleroderma. *The Journal of investigative dermatology*. 1999; 112:456–462. [PubMed: 10201529]
43. Fuxa M, Skok J, Souabni A, Salvaggio G, Roldan E, Busslinger M. Pax5 induces V-to-DJ rearrangements and locus contraction of the immunoglobulin heavy-chain gene. *Genes Dev*. 2004; 18:411–422. [PubMed: 15004008]
44. Vieira P, Rajewsky K. The half-lives of serum immunoglobulins in adult mice. *European journal of immunology*. 1988; 18:313–316. [PubMed: 3350037]
45. Arnold LW, Pennell CA, McCray SK, Clarke SH. Development of B-1 cells: segregation of phosphatidyl choline-specific B cells to the B-1 population occurs after immunoglobulin gene expression. *The Journal of experimental medicine*. 1994; 179:1585–1595. [PubMed: 8163938]
46. Hardy RR, Wei CJ, Hayakawa K. Selection during development of VH11+ B cells: a model for natural autoantibody-producing CD5+ B cells. *Immunological reviews*. 2004; 197:60–74. [PubMed: 14962187]
47. Cambier JC, Gauld SB, Merrell KT, Vilen BJ. B-cell anergy: from transgenic models to naturally occurring anergic B cells? *Nature reviews. Immunology*. 2007; 7:633–643.

48. Notley CA, Baker N, Ehrenstein MR. Secreted IgM enhances B cell receptor signaling and promotes splenic but impairs peritoneal B cell survival. *Journal of immunology*. 2010; 184:3386–3393.
49. Nguyen XH, Lang PA, Lang KS, Adam D, Fattakhova G, Foger N, Kamal MA, Prilla P, Mathieu S, Wagner C, Mak T, Chan AC, Lee KH. Toso regulates the balance between apoptotic and nonapoptotic death receptor signaling by facilitating RIP1 ubiquitination. *Blood*. 2011; 118:598–608. [PubMed: 21613257]
50. Molina H, Holers VM, Li B, Fung Y, Mariathasan S, Goellner J, Strauss-Schoenberger J, Karr RW, Chaplin DD. Markedly impaired humoral immune response in mice deficient in complement receptors 1 and 2. *Proceedings of the National Academy of Sciences of the United States of America*. 1996; 93:3357–3361. [PubMed: 8622941]
51. Sakamoto N, Shibuya K, Shimizu Y, Yotsumoto K, Miyabayashi T, Sakano S, Tsuji T, Nakayama E, Nakauchi H, Shibuya A. A novel Fc receptor for IgA and IgM is expressed on both hematopoietic and non-hematopoietic tissues. *European journal of immunology*. 2001; 31:1310–1316. [PubMed: 11465087]
52. Honda S, Kurita N, Miyamoto A, Cho Y, Usui K, Takeshita K, Takahashi S, Yasui T, Kikutani H, Kinoshita T, Fujita T, Tahara-Hanaoka S, Shibuya K, Shibuya A. Enhanced humoral immune responses against T-independent antigens in Fc alpha/muR-deficient mice. *Proceedings of the National Academy of Sciences of the United States of America*. 2009; 106:11230–11235. [PubMed: 19549827]
53. Honjo K, Kubagawa Y, Jones DM, Dizon B, Zhu Z, Ohno H, Izui S, Kearney JF, Kubagawa H. Altered Ig levels and antibody responses in mice deficient for the Fc receptor for IgM (FcmuR). *Proceedings of the National Academy of Sciences of the United States of America*. 2012; 109:15882–15887. [PubMed: 22984178]
54. Herzog S, Reth M, Jumaa H. Regulation of B-cell proliferation and differentiation by pre-B-cell receptor signalling. *Nature reviews. Immunology*. 2009; 9:195–205.
55. Kantor AB, Herzenberg LA. Origin of murine B cell lineages. *Annual review of immunology*. 1993; 11:501–538.
56. Deenen GJ, Kroese FG. Murine peritoneal Ly-1 B cells do not turn over rapidly. *Annals of the New York Academy of Sciences*. 1992; 651:70–71. [PubMed: 1376089]
57. Wardemann H, Boehm T, Dear N, Carsetti R. B-1a B cells that link the innate and adaptive immune responses are lacking in the absence of the spleen. *The Journal of experimental medicine*. 2002; 195:771–780. [PubMed: 11901202]
58. Montecino-Rodriguez E, Dorshkind K. B-1 B cell development in the fetus and adult. *Immunity*. 2012; 36:13–21. [PubMed: 22284417]

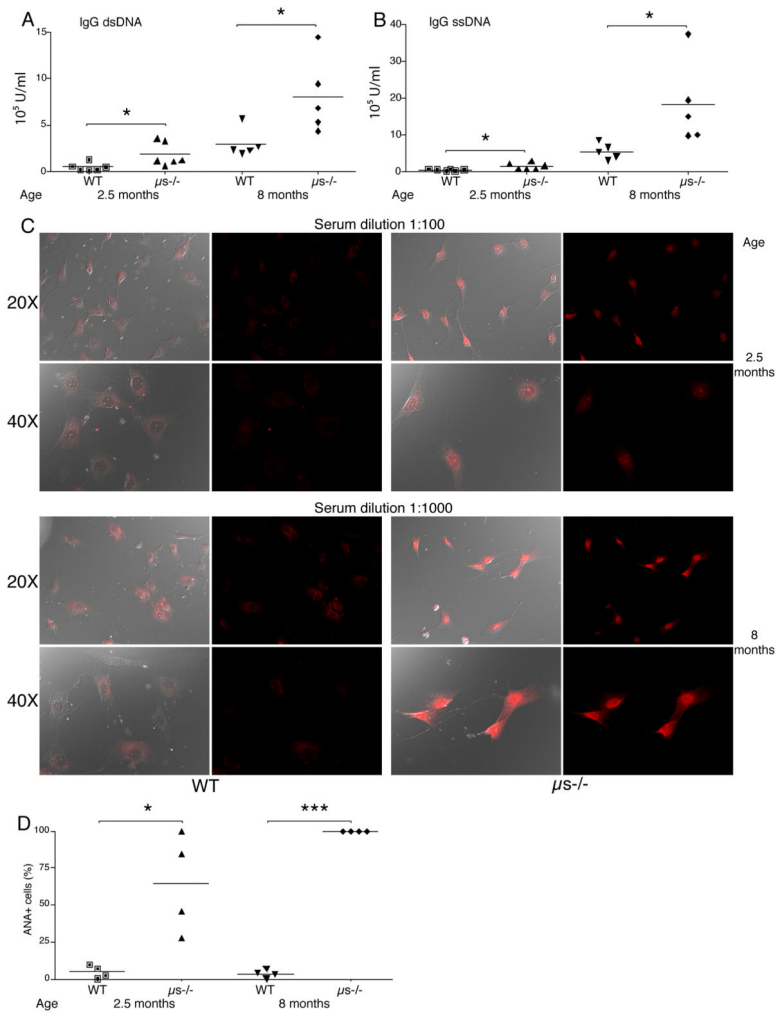


Figure 1. Strong production of anti-DNA and ANA serum autoantibodies in $\mu S^{-/-}$ mice
 (A and B) Shown are relative units (A) anti-dsDNA IgG and (B) anti-ssDNA IgG in WT and $\mu S^{-/-}$ mice at indicated ages as measured by ELISA. Each symbol represents values for a single mouse, horizontal bars indicate mean for the group (n=5 – 6/group). (C) Detection of antinuclear antibodies (ANA) via fluorescent staining of mouse 3T3 cells with serum from young and aged WT and $\mu S^{-/-}$ mice. Representative images are shown. Left panels shows the overlay images with DIC outlining the cells and fluorescent red staining for IgG, right panels shows images with fluorescent red staining for IgG only. White bars indicate 25- μ m scale bars. (D) Shown are frequencies of cells stained with diluted sera as indicated, calculated from counting total cells and stained nuclei from randomly chosen images (n=20–100 cells per slide). Data are representative of three (A, B) or two (C, D) independent experiments. Group-wise comparisons were conducted using Student’s t test: *p<0.05, **p<0.005, ***p<0.0005.

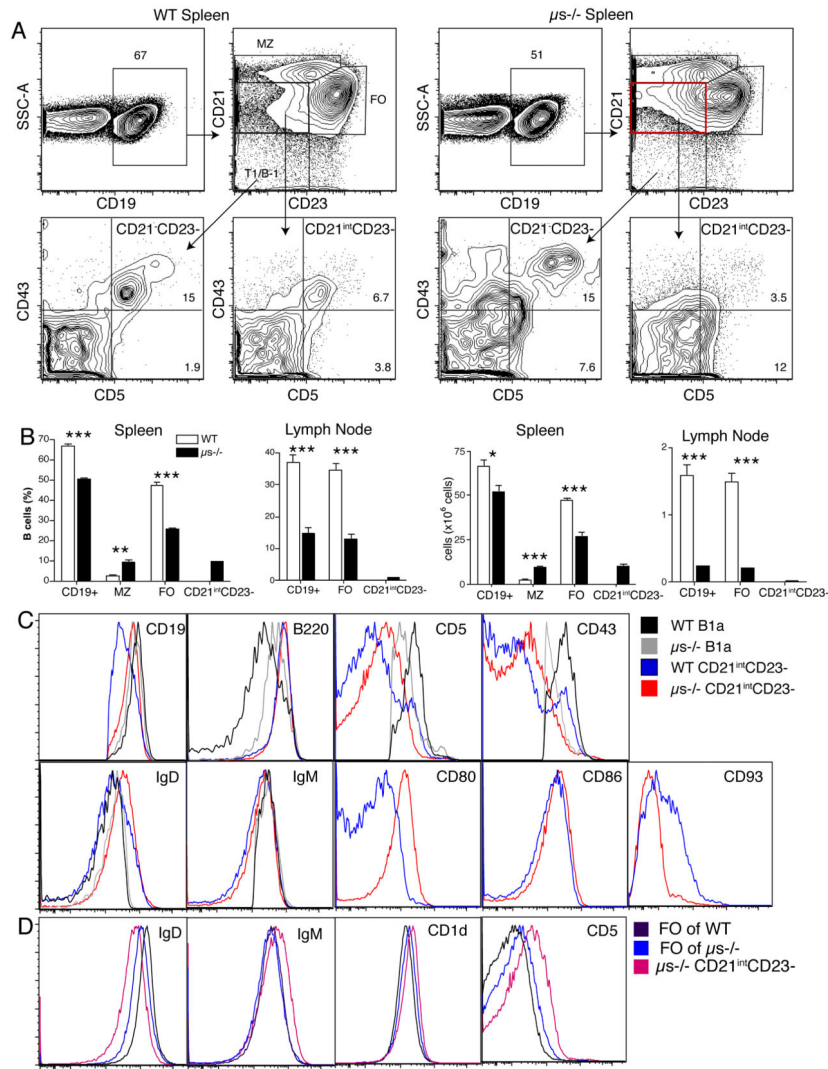


Figure 2. Presence of unusual CD5⁺ CD21^{int} CD23⁻ B cell subsets in lymph tissues of $\mu s^{-/-}$ mice (A) Shown are 5% contour plot with outliers of a representative spleen sample (n=4) from WT (left) and $\mu s^{-/-}$ mice (right) analyzed by flow cytometry after exclusion of dead cells. Boxes and arrows indicate gating strategy. Identified subsets among CD19⁺ B cells: CD21^{hi} CD23⁻ marginal zone B cells (MZ), CD21^{int} CD23⁺ follicular B cells (FO), CD21^{int} CD23⁻, unknown B cell subset, and CD21⁻ CD23⁻ transitional/B-1 cells. CD21^{int} CD23⁻ and CD21⁻ CD23⁻ subsets were gated on CD43 and CD5 to identify CD43⁺ CD5⁺ (B-1a), CD43⁻ CD5⁺. (B) Bar graphs summarize the mean frequencies \pm SD and total numbers of different B cell subsets in spleen and lymph nodes of WT and $\mu s^{-/-}$ mice (n=4 per group). (C and D) Overlay histograms comparing CD21^{int} CD23⁻ B cells from $\mu s^{-/-}$ and WT mice identifies CD21^{int} CD23⁻ B cells as a unique cell subset not present in WT mice, as cells with that phenotype of WT mice are a mix of B-1 and immature B cells. Data are representative of three independent experiments.

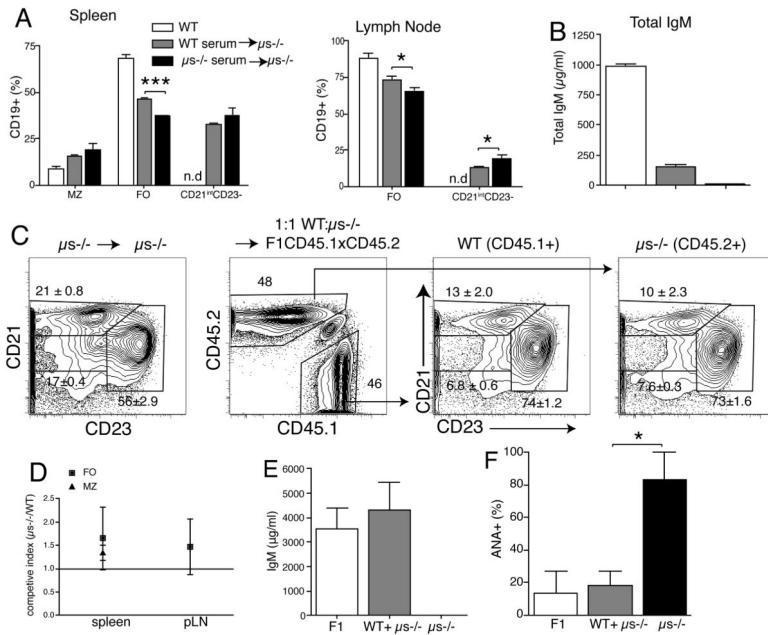


Figure 3. B cell development from $\mu s^{-/-}$ bone marrow is normal in the presence of sIgM
 (A) Groups of $\mu s^{-/-}$ mice (n=3 – 4) were given WT or $\mu s^{-/-}$ serum. Mock-treated WT mice served as controls. Data are from FACS-analysis used to determine the frequencies \pm SD of the different B cell subsets in lymph tissue as shown in Fig. 2; n.d, not detected. (B) Serum concentrations of sIgM in groups of mice outlined in (A). (C) Mixed bone marrow chimeras established with equal numbers of WT (CD45.1) and $\mu s^{-/-}$ (CD45.2) bone marrow transferred into lethally-irradiated (CD45.1xCD45.2) F1 mice (n=6). Control group is $\mu s^{-/-}$ BM transferred into $\mu s^{-/-}$ mice (left panel). Shown are contour plots with outliers from mice 10 weeks after transfer, after gating on live CD19+ splenocytes. WT (CD45.1) and $\mu s^{-/-}$ (CD45.2) B cells in the chimeras were gated on CD21 and CD23 to identify B cell subsets. Numbers indicate frequencies \pm SD of B cell subsets. (D) Frequencies of WT and $\mu s^{-/-}$ origin B cells were calculated using a competitive index derived from the frequencies measured by FACS. Competitive index is the ratio of $\mu s^{-/-}$ to WT B cells before and after BM transfer. (E) Mean serum concentrations \pm SD of sIgM. (F) Shown are ANA antibody levels as determined by the frequencies of 3T3 cells stained with serum from the mixed bone-marrow chimeras. The horizontal line indicates mean for each group. Data are representative of two independent experiments (A–E).

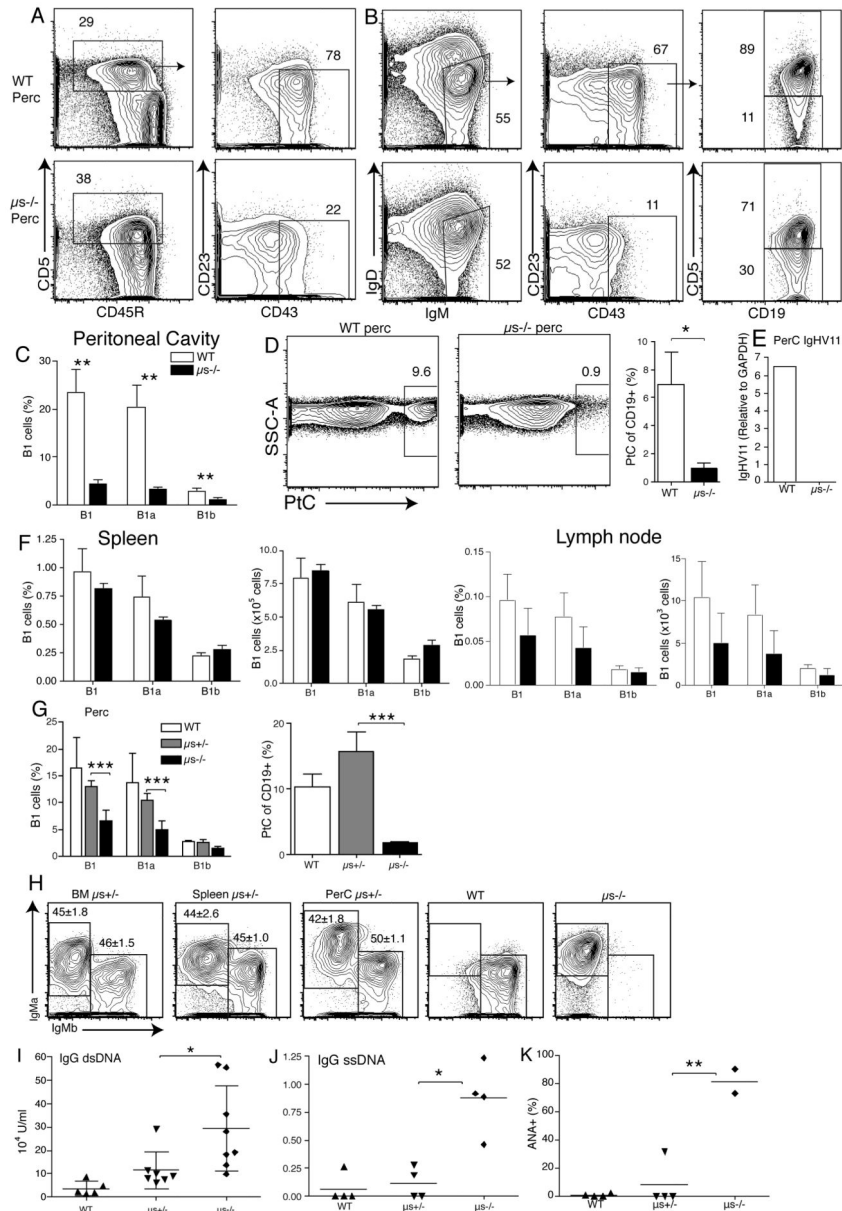


Figure 4. Lack of B-1 cells in peritoneal cavity but not spleen of μ S $^{-/-}$ mice

(A) Shown are 5% contour plots with outliers gated on live CD19⁺ peritoneal cavity B cells from WT and μ S $^{-/-}$ mice (n=3–5 mice/group), identifying CD5⁺CD23⁻ cells that differ in CD43 expression. (B) B-1 cells were further identified by gating on IgM^{hi} IgD^{lo} CD23⁻ CD43⁺ and CD5^{+/-} (B-1a/B-1b). (C) Bar chart indicating mean frequencies \pm SD IgM^{hi} IgD^{lo} CD23⁻ CD43⁺ CD5^{+/-} B-1 cells in peritoneal cavity, spleen and lymph nodes of indicated mice. (D) Left, shown are 5% contour plots with outliers of live CD19⁺ B cells binding to phosphatidylcholine (PtC)-containing liposomes. Right, mean frequencies \pm SD PtC-binding B-1 cells. (E) Relative expression of IgHV11 of purified CD23⁻ B cells from WT and μ S $^{-/-}$ pleural cavity determined by qRT-PCR (n=3 per group). (F) Frequencies of B-1 cells and frequencies of PtC-binders in peritoneal cavity of WT, μ S $^{+/-}$ and μ S $^{-/-}$

littermates (n=4 per group). (G) Representative FACS analysis of CD19+ IgM+ cells in bone marrow, spleen and peritoneal cavity of indicated mice (IgM-a, μ s allele and IgM-b, WT allele). Numbers indicate mean frequencies \pm SD for the group (n=3–5). (H and I) IgG anti-dsDNA (H) and IgG anti-ssDNA (I) in sera of indicated mice as measured by ELISA. (J) Anti-nuclear antibody levels in sera of indicated mice. Data are representative of three independent experiments (A–J)

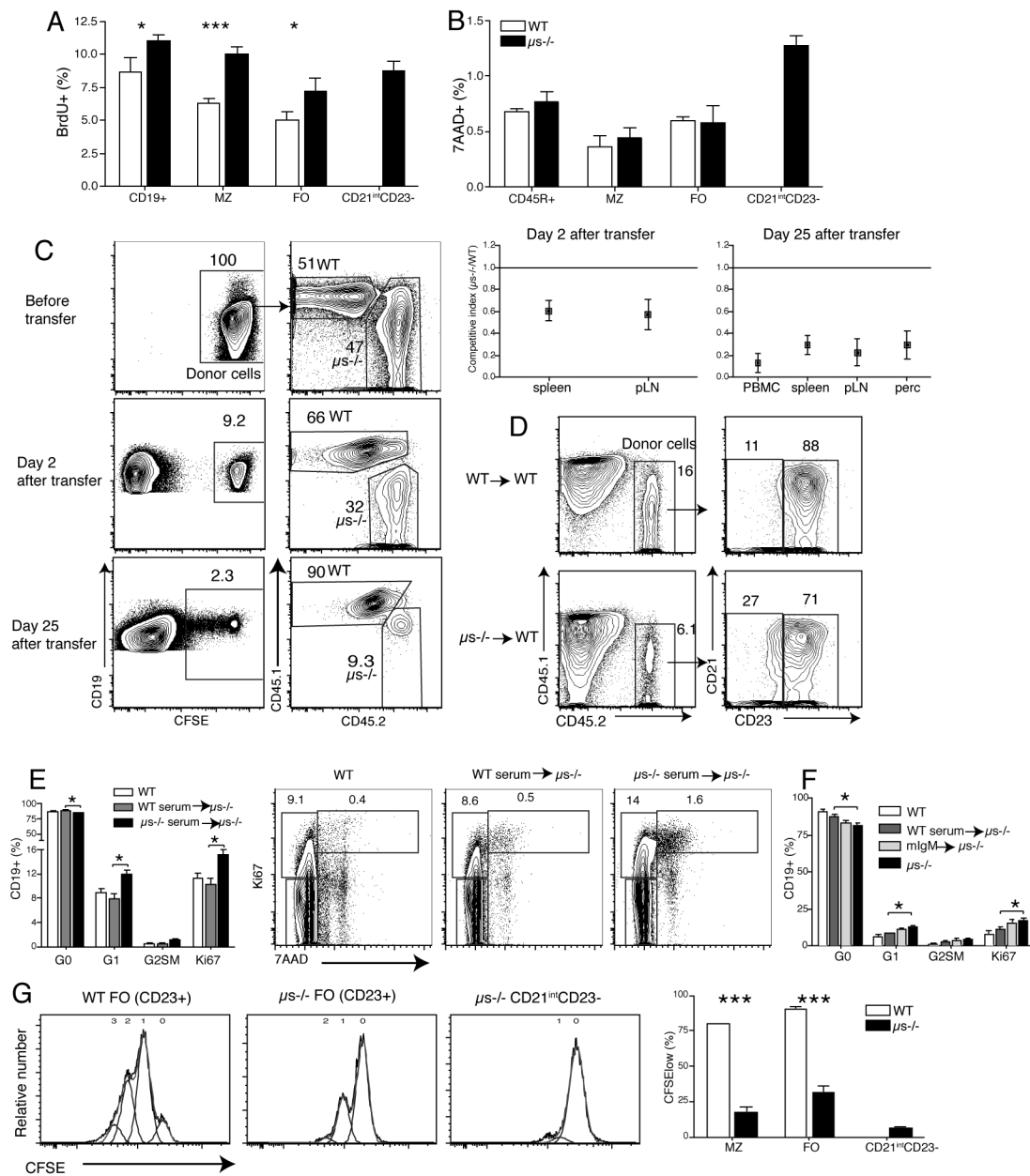


Figure 5. $\mu s^{-/-}$ CD21^{int}CD23⁻ B cells are anergic

(A) B cell proliferation was determined in WT and $\mu s^{-/-}$ mice by flow cytometry after 7 days continuous BrdU-labeling. Shown are mean frequencies \pm SD BrdU+ cells (n=4 per group). (B) Mean frequencies \pm SD of dead cells among different B cell subsets were determined by 7-AAD staining (n=4 per group). (C) Splenic B cells from WT (CD45.1) and $\mu s^{-/-}$ (CD45.2) mice were labeled with CFSE and transferred 1:1 into WT mice (n=4). Two and 25 days after transfer, the ratios of $\mu s^{-/-}$ B cells to WT B cells were determined by flow cytometry, gating on CFSE+ CD45.2 and CD45.1 cells, respectively. Competitive index is the ratio of $\mu s^{-/-}$ to WT B cells after transfer compared to that before transfer. (D) Mature B cells from WT or $\mu s^{-/-}$ B cells were transferred i.v. into WT (CD45.1) mice. Shown are

counter plot with 5% outlier after gating on live CD19⁺ lymphocytes for frequency of CD21^{int} C23⁻ and CD21^{int} CD23⁺ (FO) B cells in the spleens two days after transfer. (E and F) Groups of μ s^{-/-} mice (n = 3 or 4) were given equivalent amounts of sIgM in form of WT serum, or monoclonal IgM (mIgM). Another group received sera from μ s^{-/-} mice, PBS-treated WT and μ s^{-/-} mice served as controls. Mean frequencies \pm SD of splenic B cells in G0, G1 or G2, S, M of the cell cycle as assessed by flow cytometry via Ki67 and 7-AAD staining (n = 3–4/group). Shown are representative 5% counter plot after gating on live CD19⁺ lymphocytes for different mouse groups of treatment. (F) Shown are CFSE-histogram plots of cells stimulated in vitro with anti-IgM (20 μ g/ml) for three days. Numbers indicate rounds of proliferation. Data are representative of two independent experiments (A, B, F).

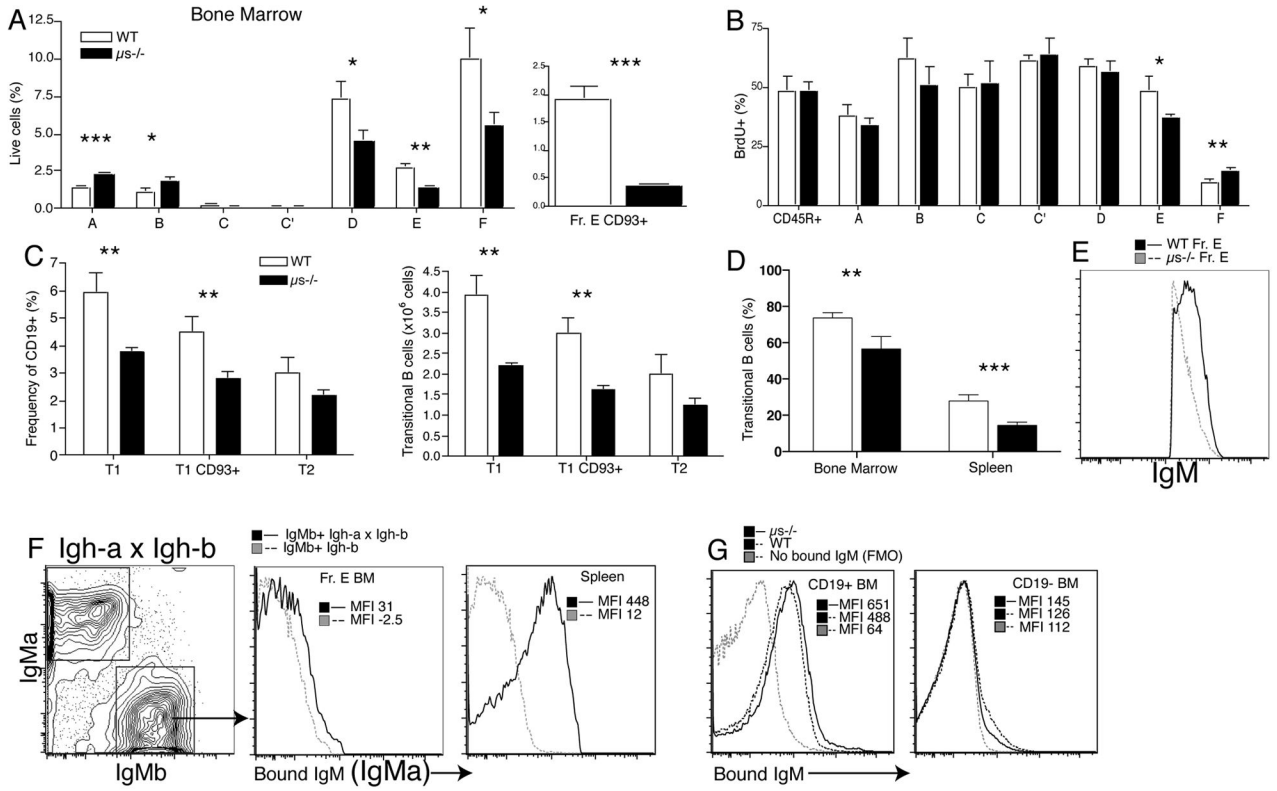


Figure 6. Lack of sIgM changes B cell development in bone marrow and periphery
 (A) Bar graph shows their mean frequencies \pm SD of B cell precursors according to Hardy (30): A, pre-pro; B, pro C; late pro; C' early pre; D late pre; E, immature; F, mature B cells. (B) Frequencies \pm SD BrdU+ cell after continuous labeling for 7 days (n=4 per group). (C) Bar graphs show the frequencies and total numbers of CD93+ transitional (T1/2) B cells in spleens of WT and μ S-/- mice. (D) Bar graph shows the frequencies \pm SD of transitional B cells (CD93+) in bone marrows and spleens 12 days after sublethal irradiated WT and μ S-/- mice. (E) Overlay histogram shows total surface IgM expression of BM Fraction E from μ S-/- and WT mice. (F) 5% contour plots of FACS staining for surface IgM-a and IgM-b of B cells from Igh-a x Igh-b heterozygous mice (n=2). Overlay histograms of sIgM-a staining, i.e. staining for sIgM bound to the cell surface of IgM-b BCR expressing CD19+ B cells from BM Fraction E and spleen, respectively. MFI, mean fluorescence intensity. (G) *In vitro* binding of sIgM to bone marrow B cells (left panel) and non-B cells (right panel) as measured by staining for sIgM using IgM allotype-specific to exclude staining for BCR. Data are representative of at least two independent experiments.

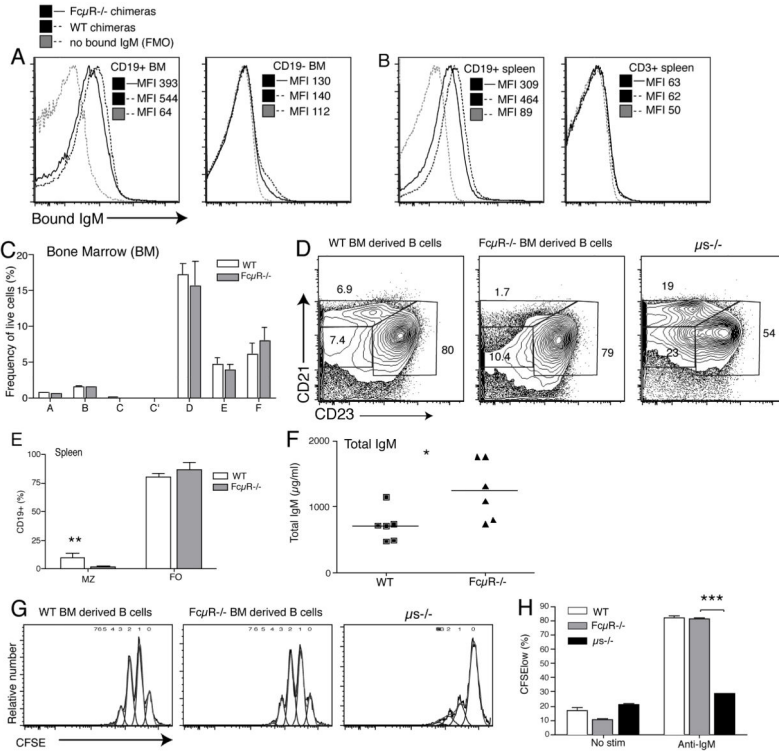


Figure 7. *FcμR*^{-/-} expression on hematopoietic cells has little effect on B cell development
 Bone marrow irradiation-chimeric mice were generated by reconstitution of lethally-irradiated C57BL/6 (CD45.1) mice with bone marrow from either wildtype or *μs*^{-/-} C57BL/6 (CD45.2) mice (n = 6/group). Shown are overlay histograms for sIgM-binding from (A) bone marrow and (B) spleen CD19⁺ B cells (left panels and non-B cells (right panels) from wildtype and *FcμR*^{-/-} chimeras after incubation with allotype-mismatched sIgM. Control stains were done staining with all reagents except for anti-IgM (FMO). (C) Flow cytometric assessment of B cell development in the bone marrow according to Hardy fractionation (Supplemental Fig. 3). (D/E) Comparison of splenic B cell pools from chimeras reconstituted with *FcμR*^{-/-} or wildtype bone marrows (F) Shown are total levels serum IgM in wildtype and *FcμR*^{-/-} chimeras as measured by ELISA; * p < 0.05. (G/H) B cells isolated from spleens of indicated chimeras, or from *μs*^{-/-} mice, were stained with CFSE and stimulated with anti-IgM for 72h. Induction of B cell proliferation was defined as reduction in CFSE staining.

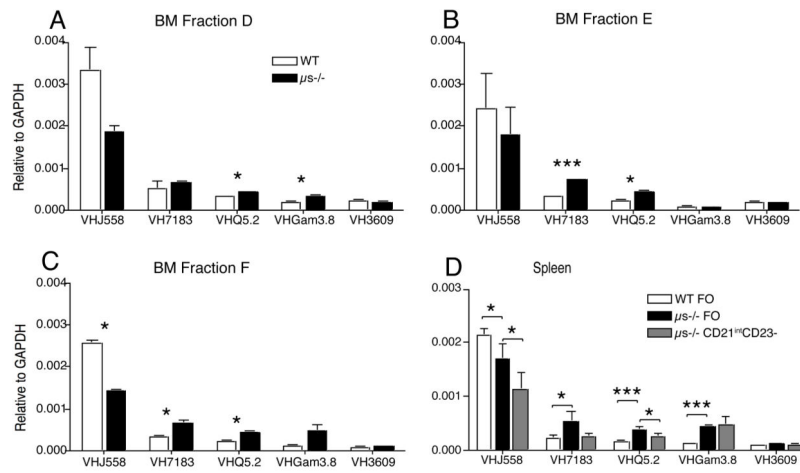


Figure 8. sIgM is required for BCR selection

(A–C) The relative expression of indicated IgHV regions among FACS-purified bone marrow B cell precursors (A) fraction D, (B) fraction E, (C) Fraction F as determined by qPCR after normalization to GAPDH (n= 6 mice per group). (D) Similar analysis of spleen follicular (FO) B cells from WT and $\mu s^{-/-}$ and $CD21^{int} CD23^{-}$ B cells from $\mu s^{-/-}$ mice. Data are representative of at least two independent experiments.